ORDER, DISORDER, AND PHASE TRANSITION IN CONDENSED SYSTEMS

Phase Diagram of the Helical Structure of a Two-Subsystem Frustrated Antiferromagnet

S. N. Martynov

Kirensky Institute of Physics, Siberian Branch, Russian Academy of Sciences, Akademgorodok, Krasnoyarsk, 660036 Russia
e-mail: UnonaV@iph.krasn.ru
Received May 20, 2008

Abstract—The expansion of the thermodynamic potential for the two-subsystem antiferromagnet with frustrated intersubsystem isotropic exchange is obtained. It is demonstrated that this expansion contains the first derivatives with respect to the antiferromagnetic vectors of the subsystems, i.e., the Lifshitz invariant. The equation for the temperature–field boundary of the helical phase for the two-subsystem frustrated antiferromagnet is derived by linearizing the variational equations for the minimum free energy within the mean-field approximation. Relationships are obtained for the critical field at $T = 0$, the angle of canting of moments of the antiferromagnetic sublattices, and the temperature of spontaneous appearance of helical ordering in the absence of an external field. It is revealed that there is a second higher temperature of formation of the helical magnetic structure induced by the magnetic field with the wave vector of the helix nonmonotonically depending on the external field. The phase boundary of the helical phase and the temperature dependence of the orientation of moments of the magnetic subsystem with weak exchange interaction are determined using numerical minimization of the free energy. It is shown that the transition to the commensurate phase is a first-order transition with a small magnetization jump. A comparative analysis of models with different spatial displacements of ions in the subsystems along the direction of the vector of the helical structure is performed. A criterion is proposed for the choice of the direction of the vector of the incommensurate magnetic structure.

PACS numbers: 75.10.-b, 75.10.Jm, 75.50.Ee, 75.50.-y

DOI: 10.1134/S1063776109010105

1. INTRODUCTION

One of the factors responsible for the formation of a magnetic structure with a period incommensurate with the crystal lattice spacing, i.e., the incommensurate magnetic structure, is the competition between magnetic interactions that orient moments differently with respect to each other. An example of these interactions is provided by antiferromagnetic exchanges with differently spaced magnetic neighbors (the ANNNI model) [1]. The mutual orientation of moments depends on the ratio between the contributions of exchanges, and the fulfillment of the threshold condition for this ratio in the simplest case leads to the formation of spiral (helical) ordering. The limiting case of the competition between the exchange interactions is a frustration, namely, a combination of competing exchanges when there exists an energy degeneracy of different states with a collinear orientation of magnetic moments. An example of this system is a triangular crystal lattice with the antiferromagnetic exchange between the nearest neighbors. The removal of this degeneracy is also accompanied by the formation of a noncollinear magnetic structure, and the choice of one of several configurations of magnetic moments with the minimum energy (ground state) is described by an additional order parameter, i.e., chirality [2–4]. The number of possible magnetic structures increases considerably for magnets formed by moments of different ions or ions in different crystalline environments, i.e., multisubsystem magnets. This is a consequence of the increase in the number of symmetry-allowed interactions and the appearance of new interactions between subsystems (intersubsystem interactions). In this case, the possibility of constructing the collinear ground state is more likely the exception. As a rule, the magnetic ordering is a result of the competition between many interactions, and it has a complex noncollinear character.

The first theoretical justification of the instability of the collinear magnetic structure with respect to small distortions of the helical type in a two-subsystem magnet was proposed by Kaplan et al. [5–9] almost simultaneously with the first experimental investigations that revealed the existence of the incommensurate magnetic structure in rare-earth and transition group metals. In the thoroughly studied structure of the AB_2O_4 cubic spinel (where A and B are magnetic ions in the tetrahedral and octahedral environments), the enhancement of the intrasubsystem antiferromagnetic exchange between the B ions to a magnitude close to that of the intersubsystem exchange leads to the formation of a ground state of the ferrimagnetic spiral type. A further increase in the relative contribution of the B exchange makes this state unstable and results in the formation of a more complex incommensurate magnetic structure,

which was not revealed. The results of the analysis of the magnetic structures of spinels are described in detail in the monographs [10, 11]. This complex character of ordering is associated with the exchange in the subsystem of B ions (B subsystem). In the B subsystem, the magnetic ions in the absence of tetrahedral distortions form structural units from regular tetrahedra (Fig. 1). The ground state of a particular individual unit is degenerate: there are topologically nonequivalent mutual orientations of moments at the vertices of tetrahedra with the same exchange interaction energy. In the cubic spinel with diamagnetic ions at the tetrahedral positions (A positions), these units form an antiferromagnetic pyrochlore lattice [12–14], in which the multiple degeneracy of the ground state leads to a magnetic behavior of the spin-liquid type. The long-range magnetic order in this system is formed only as the result of an additional lattice distortion or the existence of additional anisotropic interactions (for example, the dipole–dipole interaction) at a temperature significantly lower than the Curie–Weiss temperature [15, 16]. The geometric frustration of exchanges inside the B subsystem is responsible for the appearance of the necessary conditions for the formation of a complex (doubly modulated [8]) incommensurate magnetic structure, which is actually formed with an increase in the contribution from the exchange mentioned above. However, the main factor responsible for the formation of the helical incommensurate magnetic structure with the dominant intersubsystem exchange is a geometric frustration over the intersubsystem exchange paths.

2. MODEL

The purpose of this work is to study the influence of geometry of the frustrated intersubsystem exchange on the conditions for the formation of an incommensurate magnetic structure and to choose the direction of the vector of this structure. Investigation into the influence of the temperature and the magnetic field on the incommensurate magnetic structure is of independent interest. The difference between the effective fields acting on moments in different subsystems leads to different dependences of the subsystem magnetizations on the field and the temperature and, as a consequence, to a more complex phase diagram as compared to a homogeneous magnet. The phase boundary between commensurate and incommensurate phases deserves special attention. In particular, the analysis of the field and temperature dependences of the vector of the incommensurate magnetic structure and the net magnetization in the vicinity of this boundary for the copper metaborate CuB_2O_4 permitted a conclusion on the frustration mechanism of formation of a helical structure in the two-subsystem antiferromagnet under consideration [17]. In the CuB_2O_4 compound, all exchange interactions occur through the boron–oxygen tetrahedra, which results in considerable extension and branching of exchange bonds. As a result, apart from

AB_2O_4

A
B
O
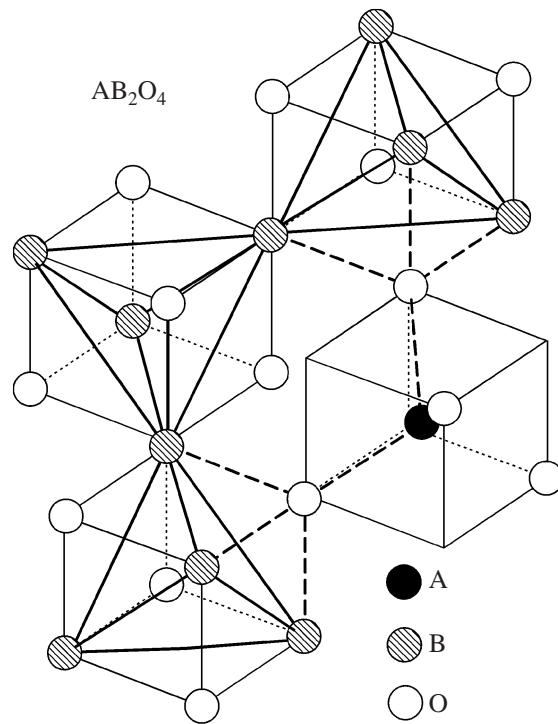
Fig. 1. Fragment of the crystal structure of the cubic spinel. Solid lines indicate the exchange inside the B subsystem. Dashed lines represent the frustrated intersubsystem exchange paths.

the exchanges between the nearest and next-nearest magnetic neighbors in one of the subsystems, there exist three different paths of the indirect intersubsystem exchange. This complicates the elucidation of the influence exerted by the geometry of the exchange interaction on the formation of the incommensurate magnetic structure. Our analysis will be performed in terms of the simplest Hamiltonian (1), which contains one type of exchange interaction within each subsystem with the constants J^A and J^B and one type of intersubsystem interaction with the constant J^{AB}; that is,

$$H = \mathbf{h}\left(\sum_i \mathbf{S}_i^A + \sum_j \mathbf{S}_j^B\right) + J^A \sum_{ii'} \mathbf{S}_i^A \cdot \mathbf{S}_{i'}^A$$

$$+ J^B \sum_{jj'} \mathbf{S}_j^B \cdot \mathbf{S}_{j'}^B + J^{AB} \sum_{ij} \mathbf{S}_i^A \cdot \mathbf{S}_j^B, \qquad (1)$$

where $\mathbf{h}$ is the external magnetic field, and $\mathbf{S}_i^A$ and $\mathbf{S}_i^B$ are the spins of the A and B subsystems, respectively. The necessary condition for the existence of the incommensurate magnetic structure is the spatial displacement of coordinates of ions in different subsystems with respect to each other in the direction of the vector $\mathbf{k}$ of the helix. In order to elucidate the influence of this factor, we compare two models with different displacements $\Delta c = (2l - 1)c/2$ ($l = 1, 2$), where c is the distance
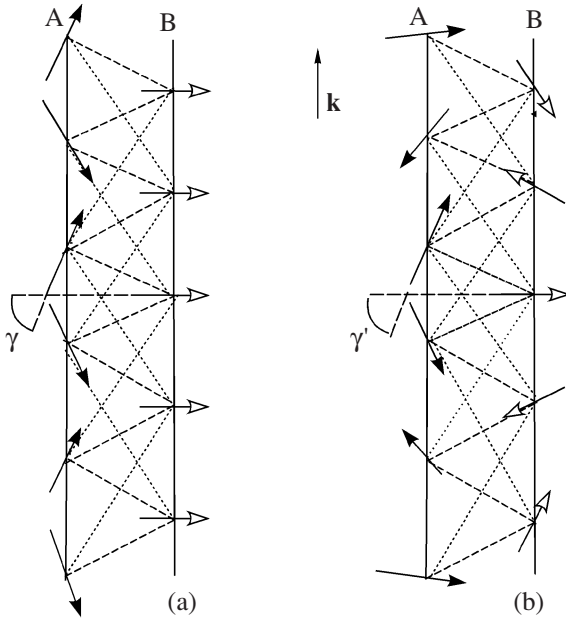
Fig. 2. (a) Yafet–Kittel ferrimagnetic and (b) helical structures. Solid lines indicate the exchange inside the subsystems. Dashed and dotted lines represent the intersubsystem exchange with the nearest ($l = 1$) and next-nearest ($l = 2$) neighbors, respectively.

between the ions inside the A subsystem with the strongest exchange.

3. GROUND STATE

The threshold conditions for the magnitudes of the exchanges at which there can appear a helical structure in the case of different intersubsystem displacements in zero external field $h = 0$ can be easily evaluated by comparing the exchange energies of the helical structure and the Yafet–Kittel ferrimagnetic structure (Fig. 2). A similar procedure for $l = 1$ and $J^A = J^B$ was used by Zhang et al. [18]; however, according to the latter equality, the energy of the helical structure was compared with the energy of antiferromagnetically ordered subsystems.

The minimization of the exchange energy of spin pairs of different subsystems for each phase,

$$E_F^{1+1} = J^A S_A^2 \cos 2\gamma + J^B S_B^2 + 2 J^{AB} S_A S_B \cos\gamma,$$

$$E_S^{1+1} = J^A S_A^2 \cos 2\gamma' + J^B S_B^2 \cos 2\gamma'$$

$$+ 2 J^{AB} S_A S_B \cos(2l - 1)\gamma',$$

with respect to the angles γ and γ' of the relative orientation and comparison of these energies allow us to

obtain different conditions for the formation of the helical structure:

$$l = 1, \quad J^B > 0 \ (AF),$$

$$(J^{AB})^2 S_B^2 < 4 J^A (J^A S_A^2 + J^B S_B^2),$$

$$J^B < 0 \ (F), \quad (J^{AB})^2 S_B^2 > 4 J^A (J^A S_A^2 + J^B S_B^2), \tag{2}$$

$$l = 2, \quad J^A \gg J^{AB}, J^B, \quad J^B J^A > -2(J^{AB})^2.$$

In the presence of the dominant antiferromagnetic (AF) exchange in one of the subsystems (A), the ferromagnetic (F) interaction inside the second subsystem ($J^B < 0$) always stabilizes the commensurate Yafet–Kittel phase at $l = 1$ and, beginning with some threshold value of J^B, at $l = 2$. If the exchange in the second subsystem (B) is antiferromagnetic ($J^B > 0$), the helical structure will always have a lower energy. It is important to note that these conditions do not depend on the sign of the intersubsystem exchange and, at $l = 2$, do not contain spins S^A and S^B: when the threshold conditions are fulfilled, the helical structure is formed immediately after the appearance of the net magnetization in the B subsystem with weak exchange.

4. THE LIFSHITZ INVARIANT

In the phenomenological description of the incommensurate magnetic structure, it is important to reveal whether the expansion of the thermodynamic potential in the vicinity of the phase transition (the Ginzburg–Landau potential) contains terms linear in the spatial derivatives of the order parameter [1]. For a two-subsystem magnet, it is also important to determine what combinations of the order parameters of the subsystems are formed by these invariants. This affects the further analysis of the stability and the type of the incommensurate magnetic structure. The symmetry analysis of this expansion for the CuB_2O_4 compound [19] demonstrated that the corresponding invariant can be obtained as a combination of components of the order parameters of different subsystems. This indicates that the mechanism responsible for the formation of the incommensurate magnetic structure in the copper metaborate is the intersubsystem interaction. However, the antisymmetric exchange (the Dzyaloshinskii–Moriya interaction [20, 21]) between moments of different subsystems, which, as rule, is responsible for the presence of the Lifshitz invariant, does not lead to gradient terms in the case of the CuB_2O_4 compound [17].

The gradient term of the thermodynamic potential can be obtained for the frustrated symmetric intersubsystem exchange described by Hamiltonian (1) upon continual transformation by expanding the classical moments $S_{r\pm a}^A$ and $S_{r\pm a}^B$. For one moment of the A sub-

system, the expression for the energy density of the intersubsystem symmetry exchange has the form

$$\varepsilon_{AB}^{A1} = \frac{1}{2}J_{AB}[\mathbf{S}_r^{A1} \cdot (\mathbf{S}_{r-a}^{B1} + \mathbf{S}_{r+a}^{B2})]$$

$$= \frac{1}{2}J_{AB}\mathbf{S}_r^{A1} \cdot \left[\mathbf{S}_r^{B1} + \mathbf{S}_r^{B2} + a\left(\frac{\partial \mathbf{S}_r^{B2}}{\partial r} - \frac{\partial \mathbf{S}_r^{B1}}{\partial r}\right)\right.$$

$$\left. + \frac{a^2}{2}\left(\frac{\partial^2 \mathbf{S}_r^{B2}}{\partial r^2} + \frac{\partial^2 \mathbf{S}_r^{B1}}{\partial r^2}\right)\right].$$

After summation over four moments of the sublattices of both subsystems and subsequent introduction of the ferromagnetic and antiferromagnetic vectors, we obtain the energy density in the following form:

$$\sum_{AB}\varepsilon_{AB} = J_{AB}\left\{(\mathbf{S}_r^{A1} + \mathbf{S}_r^{A2}) \cdot (\mathbf{S}_r^{B1} + \mathbf{S}_r^{B2})\right.$$

$$+ \frac{a}{2}\left[(\mathbf{S}_r^{A1} - \mathbf{S}_r^{A2}) \cdot \frac{\partial(\mathbf{S}_r^{B2} - \mathbf{S}_r^{B1})}{\partial r}\right.$$

$$\left. - (\mathbf{S}_r^{B2} - \mathbf{S}_r^{B1}) \cdot \frac{\partial(\mathbf{S}_r^{A1} - \mathbf{S}_r^{A2})}{\partial r}\right]$$

$$+ \frac{a^2}{4}\left[(\mathbf{S}_r^{A1} + \mathbf{S}_r^{A2}) \cdot \frac{\partial^2(\mathbf{S}_r^{B1} + \mathbf{S}_r^{B2})}{\partial r^2}\right. \tag{3}$$

$$\left.\left. + (\mathbf{S}_r^{B1} + \mathbf{S}_r^{B2}) \cdot \frac{\partial^2(\mathbf{S}_r^{A1} + \mathbf{S}_r^{A2})}{\partial r^2}\right]\right\}$$

$$= J_{AB}\left[\mathbf{M}_r^A \cdot \mathbf{M}_r^B + \frac{a}{2}\left(\mathbf{L}_r^B \cdot \frac{\partial \mathbf{L}_r^A}{\partial r} - \mathbf{L}_r^A\frac{\partial \mathbf{L}_r^B}{\partial r}\right)\right.$$

$$\left. + \frac{a^2}{4}\left(\mathbf{M}_r^A \cdot \frac{\partial^2 \mathbf{M}_r^B}{\partial r^2} + \mathbf{M}_r^B \cdot \frac{\partial^2 \mathbf{M}_r^A}{\partial r^2}\right)\right],$$

where

$$\mathbf{M}_r^A = \mathbf{S}_r^{A1} + \mathbf{S}_r^{A2}, \quad \mathbf{M}_r^B = \mathbf{S}_r^{B1} + \mathbf{S}_r^{B2},$$

and

$$\mathbf{L}_r^A = \mathbf{S}_r^{A1} - \mathbf{S}_r^{A2}, \quad \mathbf{L}_y^B = \mathbf{S}_r^{B1} - \mathbf{S}_r^{B2}$$

are the ferromagnetic and antiferromagnetic vectors for each subsystem.

Therefore, the Lifshitz invariant constructed on the antiferromagnetic vectors of both subsystems appears in the thermodynamic potential. It should be noted that the absence of the inversion center as a necessary condition for the existence of this invariant is automatically fulfilled for the interaction between moments of differ-

ent subsystems. The existence of gradient terms for the symmetric exchange in the vicinity of the corresponding commensurate vector of the magnetic structure is demonstrated in [1]. The phenomenological analysis of the frustrated distorted triangular structure was performed using the Lifshitz invariant appearing upon deviation from 120-degree orientation of magnetic moments with the formation of the incommensurate magnetic structure [22].

For the crystal structure that allows for the occurrence of antisymmetric exchange that results in the helical canting of moments, we have

$$H_D = \mathbf{D} \cdot \sum_r \mathbf{S}_r \times \mathbf{S}_{r+a}, \tag{4}$$

where $\mathbf{D}$ is the Dzyaloshinskii–Moriya interaction constant. The corresponding expansion of the moments of two antiferromagnetic sublattices upon continual transformation leads to the energy density in the form

$$\varepsilon \approx 2D^z a\left(S_r^{1x}\frac{\partial S^{2y}}{\partial r} - S_r^{1y}\frac{\partial S^{2x}}{\partial r}\right)$$

$$= 2D^z a\left(S_r^{2x}\frac{\partial S^{1y}}{\partial r} - S_r^{2y}\frac{\partial S^{1x}}{\partial r}\right) \tag{5}$$

$$= \mathbf{D} \cdot \left(\mathbf{M} \times \frac{\partial \mathbf{M}}{\partial r} - \mathbf{L} \times \frac{\partial \mathbf{L}}{\partial r}\right)\frac{a}{2}.$$

For the antiferromagnet, the inequality $\mathbf{M} \ll \mathbf{L}$ is satisfied and the ferromagnetic term can be ignored. Taking into account the external formal similarity of invariants (3) and (5) with the first derivatives, it should be noted that relationship (3) involves the scalar products of the antiferromagnetic vectors and their derivatives for different subsystems, whereas expression (5) for the relativistic mechanism includes the vector product. The magnitude of the coefficient J_{AB} of the gradient in expression (3) is not limited, whereas interaction (4) is characterized by the corresponding limitation

$$D \sim \frac{\Delta g}{g}J, \tag{6}$$

where Δg is the deviation of the g factor from the pure spin value. The quantity $\Delta g/g$ imposes substantial limitations on the wave vector of the helix for ions in the S state, for which this deviation is insignificant. In actual fact, the relative deviation of the g factor determines the upper limit of the wave vector of the incommensurate magnetic structure formed according to the relativistic mechanism. For the incommensurate magnetic structure with the frustration mechanism, this limit is absent.

5. FREE ENERGY

The separation of the magnet into the subsystems is convenient primarily for describing its properties at a
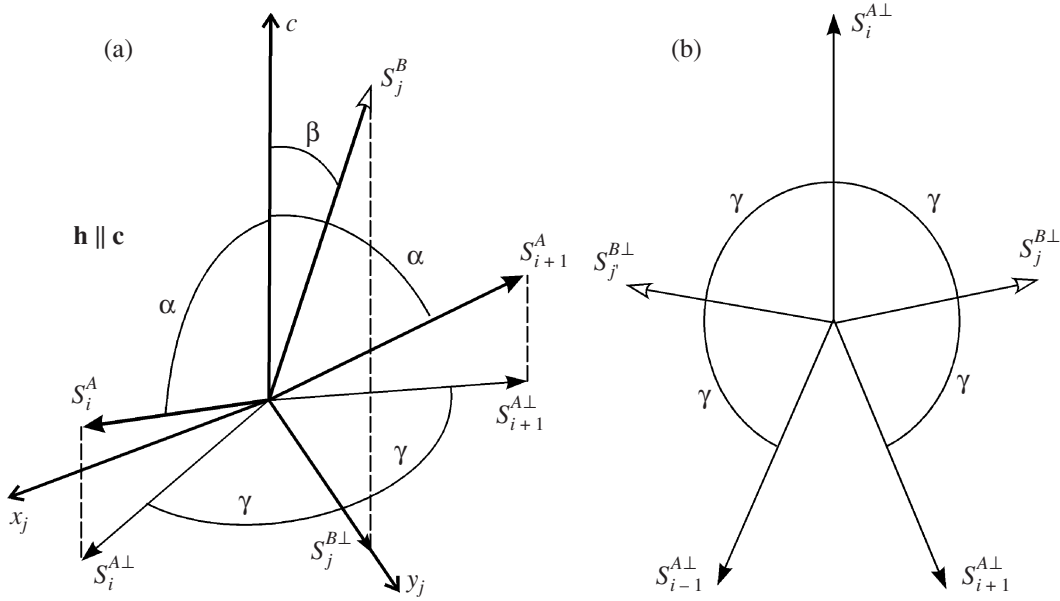
Fig. 3. Local orientations of (a) the spins $S_j^{A,B}$ in the space and (b) their projections $S_j^{A\perp}$ and $S_j^{B\perp}$ in the $x_j y_j$ plane.

finite temperature in the mean-field approximation; that is,

$$V_{ij}\mathbf{S}_i \cdot \mathbf{S}_j = \mathbf{h}_a^{\text{eff}} \cdot \mathbf{S}_i + \mathbf{h}_b^{\text{eff}} \cdot \mathbf{S}_j,$$

$$\mathbf{h}_{a,b}^{\text{eff}} = f(\langle \mathbf{S}_i \rangle_T, \langle \mathbf{S}_j \rangle_T, \varphi_i, \varphi_j, h).$$

Here, V_{ij} involves all interactions included by the model and the effective fields $\mathbf{h}_{a,b}^{\text{eff}}$ acting on the moments of each subsystem depend on the average values and the angles $\varphi_{i,j}$ of the mutual orientation of the interacting moments. In this case, the temperature dependences of the equilibrium magnetization of each moment in the mean field with the same strength in the subsystem should be identical. Therefore, the minimization of the free energy

$$F = -T\ln Z$$

with respect to the angles of the local orientation of the moments and their average values with due regard for the self-consistency (the Euler–Lagrange variational procedure) completely determines the equilibrium structure in the mean-field approximation. The simple three-dimensional helical structure is uniquely specified by three angles of the mutual orientation of the moments (the principle of "equal relative angles" [8]) (Fig. 3). The sole origin of the anisotropy in the model under consideration (relationship (1)) is an external magnetic field. This means that the antiferromagnetically ordered moments of the A subsystem always rotate perpendicular to the external field, which determines the plane of the helical structure. The moments

of the A (B) subsystem form angles $\alpha(\beta)$ with the external field. The mean-field approximation provides the additivity of the free energy with respect to the moments of the subsystems; that is,

$$F = -T\ln(Z_A Z_B) = -T(\ln Z_A + \ln Z_B),$$

where $Z_{A,B}$ are the partition functions for the spins states in the subsystem. For spin $S = 1/2$, the partition functions have the form

$$Z_{A,B} = Z_{1A,1B}^{N_{A,B}} = \left[\exp\left(\frac{h_{a,b}^{\text{eff}}}{2T}\right) + \exp\left(-\frac{h_{a,b}^{\text{eff}}}{2T}\right) \right]^{N_{A,B}},$$

where $Z_{1A,1B}$ are the partition functions for one spin of each subsystem. As a result, the free energy can be written in the form

$$F = -T(N_A \ln Z_{1A} + N_B \ln Z_{1B}) = N_A F_1,$$

$$F_1 = -T(\ln Z_{1A} + n\ln Z_{1B}), \quad n = \frac{N_B}{N_A}, \tag{7}$$

and the average magnetization of the subsystems is represented as follows:

$$S_{A,B} = \frac{1}{2}\tanh\frac{h_{a,b}^{\text{eff}}}{2T}, \tag{8}$$

$$\frac{\partial F_1}{\partial \varphi_{i,j}} = -S_A \frac{\partial h_a^{\text{eff}}}{\partial \varphi_{i,j}} - nS_B \frac{\partial h_b^{\text{eff}}}{\partial \varphi_{i,j}} = 0. \tag{9}$$

At $T = 0$, the entropy contribution vanishes and the free energy transforms into the exchange energy of the ground state.

For the model with $l = 1$, $J^A > 0$, $J^B > 0$, and $n = 1$, the effective fields are defined by the relationships

$$h_a^{\text{eff}} = h\cos\alpha - J^A S_A(\cos^2\alpha + \sin^2\alpha\cos 2\gamma)$$

$$- J^{AB}S_B(\cos\alpha\cos\beta + \sin\alpha\sin\beta\cos\gamma),$$

$$h_b^{\text{eff}} = h\cos\beta - J^B S_B(\cos^2\beta + \sin^2\beta\cos 2\gamma) \quad (10)$$

$$- J^{AB}S_A(\cos\alpha\cos\beta + \sin\alpha\sin\beta\cos\gamma).$$

Conditions (2) mean that the effects associated with the formation of the helical structure occur at temperatures considerably lower than the Néel temperature in the A subsystem with the strongest exchange interaction. Therefore, the derivative of the average magnetization of this subsystem with respect to the angles can be disregarded:

$$\frac{\partial S_{A,B}}{\partial\varphi_{i,j}} = \frac{1 - 4S_{A,B}^2}{4T}\frac{\partial h_{a,b}^{\text{eff}}}{\partial\varphi_{i,j}}, \quad \frac{\partial S_A}{\partial\varphi_{i,j}} \ll 1,$$

$$\frac{\partial S_B}{\partial\alpha} = \frac{J^{AB}S_A(\sin\alpha\cos\beta - \cos\alpha\sin\beta\cos\gamma)}{4T(1 - 4S_B^2)^{-1} + J^B(\cos^2\beta + \sin^2\beta\cos 2\gamma)}$$

$$\xrightarrow[\beta\to 0]{} J^{AB}\chi_B S_A\sin\alpha, \quad (11)$$

$$\chi_B = \left(\frac{4T}{1 - 4S_B^2} + J^B\right)^{-1}.$$

The derivative of the free energy with respect to the angles $\varphi_{i,j} = \alpha, \beta$, and γ (see expression (9)) results in three equations for the equilibrium angles. As the phase boundary is approached with an increase in the field ($h \longrightarrow h_c$), we have $\beta \longrightarrow 0$ and $\gamma \longrightarrow \pi/2$. The derivative of the free energy with respect to the angle α determines the longitudinal magnetization of the A subsystem:

$$\left.\frac{\partial F_1}{\partial\alpha}\right|_{\beta\to 0, \gamma\to\pi/2} = S_A\sin\alpha[h - 4J^A S_A\cos\alpha$$

$$- 2J^{AB}S_B + J^{AB}(J^{AB}S_A\cos\alpha + J^B S_B)\chi_B] = 0.$$

As a result, we obtain

$$S_A\cos\alpha = \frac{h - 2J^{AB}S_B + J^{AB}J^B S_B\chi_B}{4J^A - (J^{AB})^2\chi_B}. \quad (12)$$

At the phase boundary, we find

$$S_B = \frac{1}{2}\tanh\frac{h - J^B S_B - J^{AB}S_A\cos\alpha}{2T}. \quad (13)$$

The other two equations are linearized with respect to the small functions $\sin\beta$ and $\cos\gamma$ in the following form:

$$\left.\frac{\partial F_1}{\partial\beta}\right|_{\beta\to 0, \gamma\to\pi/2} = \sin\beta[hS_B - 4J^B S_B^2$$

$$- 2J^{AB}S_B S_A\cos\alpha$$

$$+ (J^{AB}S_A\cos\alpha + 4J^B S_B - h)\chi_B]$$

$$+ J^{AB}S_A\sin\alpha\cos\gamma$$

$$\times[2S_B - (J^B S_B + J^{AB}S_A\cos\alpha)\chi_B] = 0, \quad (14)$$

$$\left.\frac{\partial F_1}{\partial\gamma}\right|_{\beta\to 0, \gamma\to\pi/2} = S_A\sin\alpha\{J^{AB}\sin\beta[(J^B S_B$$

$$+ J^{AB}S_A\cos\alpha)\chi_B - 2S_B]$$

$$- 4J^A S_A\sin\alpha\cos\gamma\} = 0.$$

The condition for the existence of the nontrivial solutions for these variables leads to the ratio between the temperature and the field at the phase boundary

$$4J^A[hS_B - 4J^B S_B^2 - 2J^{AB}S_B S_a\cos\alpha$$

$$- (h - 4J^B S_B^2 - J^{AB}S_A\cos\alpha)$$

$$\times (J^{AB}S_A\cos\alpha + J^B S_B)\chi_B] \quad (15)$$

$$= (J^{AB})^2[2S_B - (J^{AB}S_A\cos\alpha + J^B S_B)\chi_B]^2.$$

The critical field at $T \longrightarrow 0$ can be obtained with allowance made for relationship (12) at $\chi_B \longrightarrow 0$:

$$h_c = \frac{4J^B S_B}{1 - J^{AB}/2J^A}. \quad (16)$$

It can be seen that the field of the transition to the commensurate phase coincides with the "spin-flip field" of the antiferromagnetic structure in the B subsystem and is proportional to its magnetization at low temperatures.

In the absence of the external magnetic field ($h = 0$), a flat helix with an arbitrary orientation of the plane is formed according to the isotropic model (1). It order to describe this structure, it is sufficient to set $\alpha = \beta = \pi/2$ in the effective fields (relationships (10)):

$$h_a^{\text{eff}} = -J^A S_a\cos 2\gamma - J^{AB}S_b\cos\gamma,$$

$$h_b^{\text{eff}} = -J^B S_b\cos 2\gamma - J^{AB}S_a\cos\gamma. \quad (17)$$
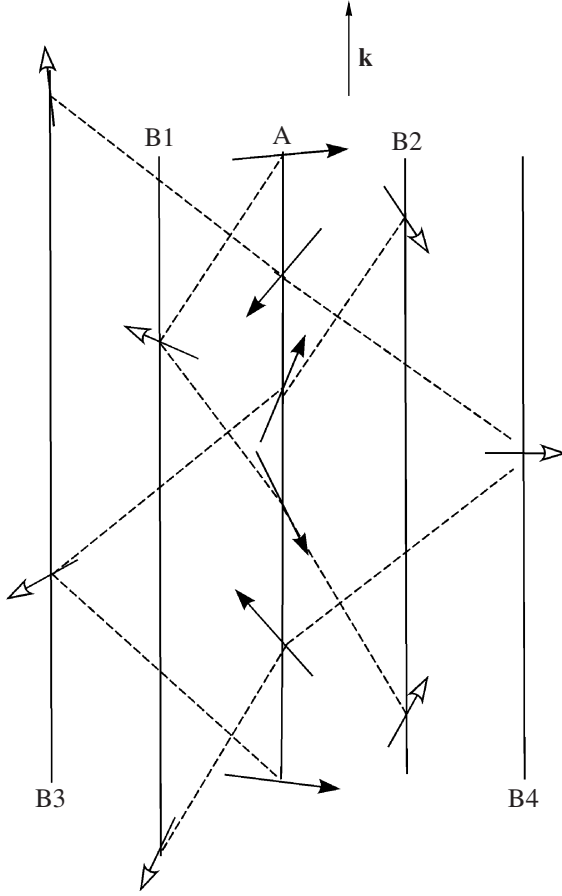
Fig. 4. Schematic diagram illustrating the exchange interactions at $l = 2$ for the CuB$_2$O$_4$ compound.

Therefore, the minimization is performed only with respect to the angle γ. At the phase boundary, we obtain

$$\frac{\partial S_B}{\partial \gamma} = \sin\gamma \frac{J^{AB}S_A + 4J^B S_B \cos\gamma}{4T(1 - 4S_B^2)^{-1} + J^B \cos 2\gamma} \tag{18}$$

$$\xrightarrow[\gamma \to \pi/2]{} J^{AB}S_A \chi_B',$$

where

$$\chi_B' = \left(\frac{4T}{1 - 4S_B^2} - J^B\right)^{-1}. \tag{19}$$

The angle between the neighboring spins in the A subsystem determines the wave vector of the helix in the absence of the external field. This angle is defined by the expression

$$\cos\gamma = -\frac{J^{AB}S_A S_B(2 + J^B \chi_B')}{4J^A S_A^2 + 4J^B S_B^2 - (J^{AB})^2 S_A^2 \chi_B'}. \tag{20}$$

At $T = 0$, we have

$$\cos\gamma_0 = -\frac{J^{AB}S_A S_B}{2(J^A S_A^2 + J^B S_B^2)}. \tag{21}$$

The last formula for identical subsystems ($J^A = J^B$, $S_A = S_B$) transforms into the result of the ANNNI model. The temperature T_{SS} of the appearance of the spontaneous magnetization in the B subsystem and, as a consequence, the formation of the helical structure in the system can be obtained from the general relationship (8) for the equilibrium magnetization S_B by substituting expressions (17) and (20):

$$S_B = \frac{1}{2}\tanh\left[\frac{S_B}{2T}\right.$$

$$\left. \times \left(J^B + \frac{(J^{AB})^2 S_A^2 (2 + J^B \chi_B')}{4J^A S_A^2 + 4J^B S_B^2 - (J^{AB})^2 S_A^2 \chi_B'}\right)\right]. \tag{22}$$

As a result, we find

$$T_{SS} = \frac{J^B}{4} + \frac{3(J^{AB})^2}{32J^A}\left[1 + \sqrt{1 + \frac{16J^A J^B}{9(J^{AB})^2}}\right]. \tag{23}$$

In order to elucidate the role of the spatial displacement of the coordinates of the interacting spins in the subsystems, let us carry out a similar analysis in the case of $l = 2$ with $\Delta c = 3c/2$. For comparison of the results of the analysis with the data for the CuB$_2$O$_4$ compound ($n = 2$), we take into account the numbers of magnetic neighbors inside the subsystems and between them,

$$z_A = 4, \quad z_B = 2, \quad z_{AB} = 4, \quad z_{BA} = 2,$$

and the corresponding distances between the interacting B spins (Fig. 4). It should be noted that the analysis of the magnetization curves in fields close to those at the phase boundary [17] demonstrated that the total mean field of the exchange interactions inside the B subsystem corresponds to the effective ferromagnetic exchange ($J^B < 0$). With allowance for this fact, the relationships for the effective fields and the longitudinal magnetization for the A subsystem take the form

$$h_a^{\text{eff}} = h\cos\alpha - 2J^A S_A(\cos^2\alpha + \sin^2\alpha\cos 2\gamma)$$

$$- 2J^{AB}S_B(\cos\alpha\cos\beta + \sin\alpha\sin\beta\cos 3\gamma),$$

$$h_b^{\text{eff}} = h\cos\beta - J^B S_B(\cos^2\beta + \sin^2\beta\cos 8\gamma) \tag{24}$$

$$- J^{AB}S_A(\cos\alpha\cos\beta + \sin\alpha\sin\beta\cos 3\gamma),$$

$$S_A\cos\alpha = \frac{h - 4J^{AB}S_B + 2J^{AB}J^B S_B\chi_B}{4J^A - (J^{AB})^2\chi_B}.$$

After minimization of the free energy, we obtain the following linearized equation for the phase boundary within the model under consideration:

$$4J^A[hS_B - 2J^{AB}S_BS_A\cos\alpha - (h - J^{AB}S_A\cos\alpha)$$

$$\times(J^{AB}S_A\cos\alpha + J^BS_B)\chi_B] \qquad (25)$$

$$= 9(J^{AB})^2[2S_B - (J^{AB}S_A\cos\alpha + J^BS_B)\chi_B]^2.$$

The expressions for the critical field, the angle of the helix at $T = 0$, and the temperature of the appearance of the spontaneous magnetization and, as a consequence, the formation of the helical phase have the form

$$h_c = \frac{8(J^{AB})^2 S_B}{J^A}, \qquad (26)$$

$$\cos\gamma_0 = -\frac{3J^{AB}S_AS_B}{2J^AS_A^2 - 32J^BS_B^2}, \qquad (27)$$

$$T_{SS} = -\frac{J^B}{4}$$
$$+ \frac{27(J^{AB})^2}{32J^A}\left[1 + \sqrt{1 - \frac{16J^AJ^B}{81(J^{AB})^2}}\right]. \qquad (28)$$

It can be seen that, unlike relationship (16) for the antiferromagnetic case, the critical field for the ferromagnetic exchange in the B subsystem is determined by the intersubsystem exchange.

6. NUMERICAL MINIMIZATION OF THE FREE ENERGY

The linearization of the variational equations for the equilibrium angles suggests the occurrence of a continuous transition from the helical phase to the commensurate Yafet–Kittel phase; i.e., the transition should be a second-order transition. In order to check this assumption, we performed the numerical minimization of the initial expression (7) for the mean field and compared the equilibrium value with the minimum free energy for the Yafet–Kittel structure. Moreover, we determined the average magnetization for the B subsystem and the wave vector of the helical structure. Figure 5 depicts the phase diagrams obtained for both models by the linearization of the variational Eqs. (15) and (25) and the temperature dependences of the magnetizations $S_B(T, h = 0)$ and $S_B(T, h_c)$ determined in zero and critical fields at the phase boundary by the numerical minimization of the free energy. For both models, the temperature T_{IS} of the formation of the incommensurate magnetic structure in the field is substantially higher than the temperature T_{SS} of the spontaneous formation of the helical structure in the absence of the field. The magnitudes of the exchange interaction constants were taken as identical for both models: $J^A =$
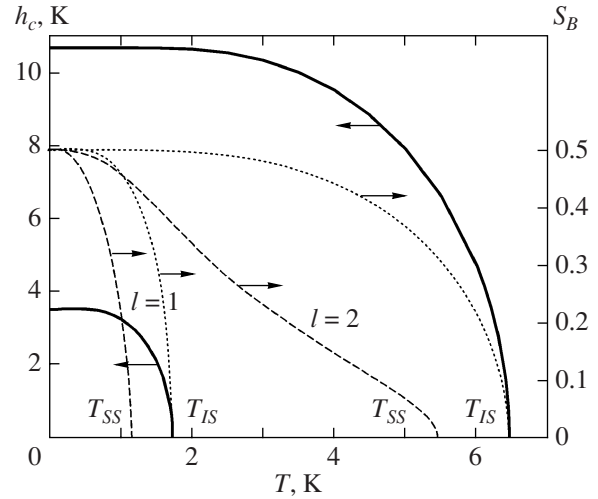
Fig. 5. Phase diagrams for the helical phase (solid lines) and the magnetization of the B subsystem in zero (dashed lines) and critical (dotted lines) fields for the models with $l = 1$ (lines at $T < 2$ K) and $l = 2$ (lines at $T < 6.5$ K).

45 K, $J^{AB} = 11.3$ K, and $J^B_{l=1} = -J^B_{l=2} = 2$ K. The magnetic fields and the exchange interaction constants are given in kelvins (1 K = 7400 Oe).

7. RESULTS AND DISCUSSION

The existence of the phase boundary associated with the magnetic field in relatively low fields determined by the antiferromagnetic exchange in the B subsystem (model with $l = 1$) or the intersubsystem exchange (model with $l = 2$) is the radical difference between the frustration and relativistic mechanisms. In the case of the relativistic mechanism, in the absence of additional anisotropic interactions, the long-period magnetic structure exists up to spin-flip fields of the antiferromagnetic structure in the A subsystem. Compared to the incommensurate magnetic structure with the competition of the exchange interactions inside one of the subsystems, the frustration mechanism is characterized by the continuous variation in the wave vector of the structure over a wide range with variations in the temperature and the field. The field dependences of the wave vector of the structure according to the calculations with the use of the numerical minimization are plotted in Fig. 6. It should be noted that the threshold condition in our case is more likely geometric in character and is absent altogether for the antiferromagnetic interactions in both subsystems. The main feature of the phase diagram (Figs. 5, 6) is that, apart from the temperature T_{SS} of the spontaneous formation of the helical phase, there exists a temperature T_{IS} below which the helical structure exists only in the external magnetic field (induced spiral (IS) phase). In the temperature range $T_{SS} < T < T_{IS}$, the field dependence of the wave vector exhibits a nonmonotonic behavior (Fig. 6). As
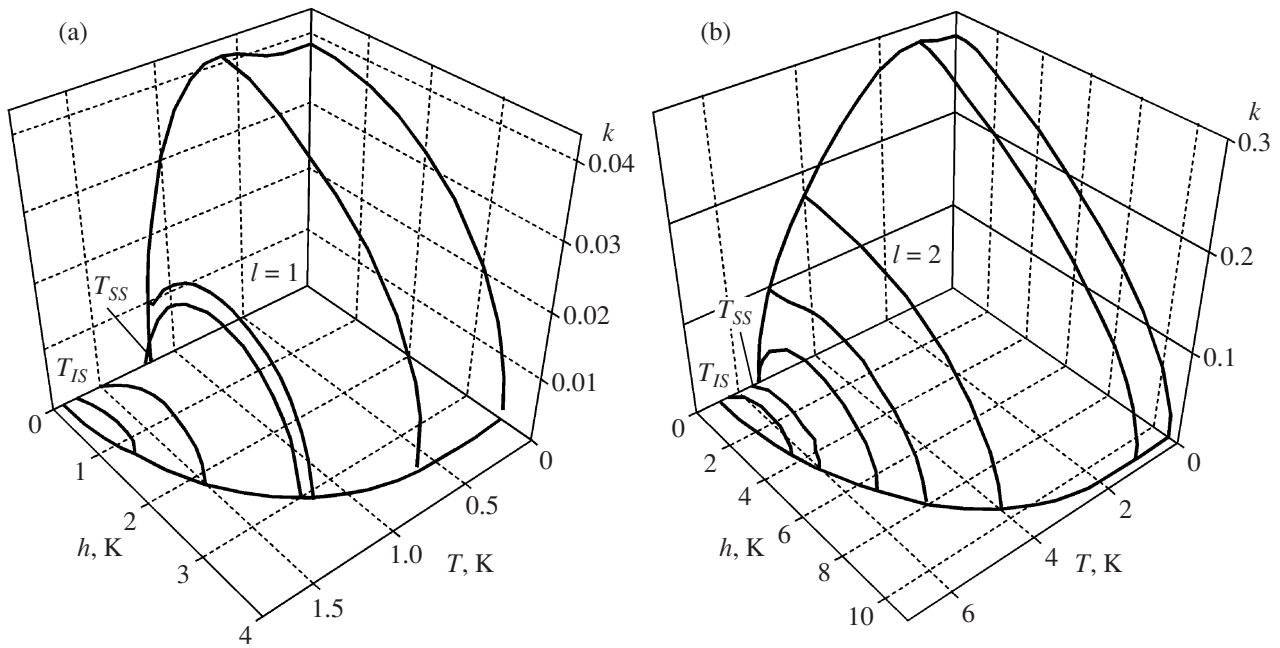
Fig. 6. Dependences of the vector of the incommensurate magnetic structure (in terms of reciprocal lattice) on the temperature and the field for the models with l = (a) 1 and (b) 2.

the field increases, the wave vector appears immediately with the appearance of the magnetization in the B subsystem ($k(h \longrightarrow 0) \longrightarrow 0$), increases to a maximum value, and then decreases to a small critical value: $k(h \longrightarrow h_{c1}) \longrightarrow k_c$. In this case, the magnetization of the B subsystem appears with an intermediate angle of the orientation with respect to the external field: $0 < \beta_0 < \pi/2$ (Fig. 7). With a further increase in the field, this
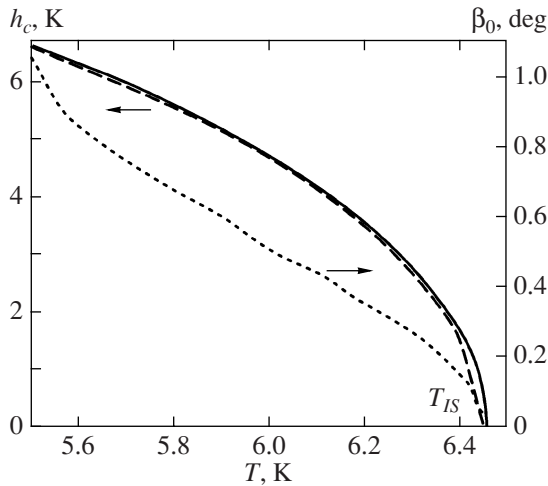
Fig. 7. Fragment of the phase boundary. h_{c1} is the critical field determined by the numerical minimization of the free energy (dashed line), h_{c2} is the critical field obtained using the linear approximation (25) (solid line), and $\beta_0(T)$ is the initial angle of orientation for the B subsystem at $l = 2$ in the helical phase induced by the magnetic field (dotted line).

angle decreases to a critical value ($\beta(h \longrightarrow h_{c1}) \longrightarrow \beta_c$) and then abruptly decreases to zero. In the phase plane, the critical parameters of the incommensurate magnetic structure determine the line where the free energy of this structure coincides with the free energy of the commensurate Yafet–Kittel structure (dotted line in Fig. 7). This phase boundary is close to the phase boundary obtained within the linearized approximation (the second-order phase transition at $h = h_{c2}$) but does not coincide with it: $h_{c1}(T) < h_{c2}(T)$. Therefore, the field-induced transition from the helical structure to the commensurate phase is a first-order phase transition and is accompanied by a stepwise decrease in the wave vector and the angle of orientation of the B subsystem to zero. The jump in the net magnetization upon this transition is small ($\Delta M < 10^{-4}M$ for the used exchange constants). The phase boundary for the CuB_2O_4 compound exhibits a double kink of the same order of magnitude [17], which can be attributed to the first order phase transition smeared over a narrow range of fields. The fact that the field-induced phase transition is the first-order transition is confirmed by the hysteresis in the appearance of the transverse magnetization in the commensurate phase [23]. The crystal structure of the CuB_2O_4 compound allows for the existence of the Dzyaloshinskii–Moriya interaction between the ions of the A subsystem. This interaction leads to the canting of the moments of the antiferromagnetic sublattices in the basal plane. Therefore, the transition in the longitudinal field from the helical phase to the commensurate Yafet–Kittel phase is accompanied by the stepwise appearance of the transverse magnetization component. The

existence of the ordering induced by the magnetic field at both $T = 0$ and finite temperatures is a common property of strongly frustrated magnets [24, 25]. A specific feature of the two-subsystem antiferromagnet is that the field-induced helical structure is a continuation of the low-temperature incommensurate magnetic structure, because the phase boundary at $h \neq 0$ between them is absent. In the given case, the magnetic field favors the appearance of magnetization in a subsystem with weak exchange and, as a consequence, the formation of the helical structure with the equilibrium intermediate angle between this magnetization and the field (Fig. 7).

In addition to the general features of the incommensurate magnetic structure formed as a result of the removal of the frustration degeneracy of states, it is important to note that the critical field, the magnitude of the wave vector of the incommensurate magnetic structure, and the transition temperature increase substantially with an increase in the spatial displacement between the ions of the interacting subsystems (expressions (16), (21), and (23) for the model with $l = 1$ and relationships (26)–(28) for the model with $l = 2$). In this case, the direction of the wave vector of the incommensurate magnetic structure is determined by the direction of the longest intersubsystem bonds as compared to the intrasubsystem exchange paths. For example, for the CuB_2O_4 compound, the bonds with $l = 2$ and 3, which also exist in the crystal structure, are longer along the c axis as compared to the bonds with $l = 1$ that are predominantly oriented in the basal plane:

$$\Delta c(l = 2, 3) > \Delta a(l = 1) > \Delta c(l = 1).$$

The preferred orientation of the paths of the exchange bonds between the ions in the A subsystem in the structure of the CuB_2O_4 compound is identical to that of the bonds with $l = 1$. Their length in the basal plane is larger than the length of the intersubsystem exchange paths. The opposite situation is observed for the tetragonal axis: the intersubsystem bonds with $l = 2$ and 3 are considerably longer than the exchange paths in this direction in the A subsystem. This provides the gain in the total energy in the case of uniform helical canting of the moments with $\mathbf{k} \parallel \mathbf{c}$.

In the aforementioned structure of the normal cubic spinel with the dominant intersubsystem exchange interaction, the direction of the longest intersubsystem bonds also coincides with the direction [110] of the vector of the helix (Fig. 8).

This criterion for the determination of the direction of the vector of the incommensurate magnetic structure is not sole or main. For example, a tetragonal distortion of the spinel can lead to the formation of the helical structure with the vector $\mathbf{k} \parallel$ [001] [7]. In any case, it is necessary to compare the magnetic structures with the minimum free (or exchange at $T = 0$) energies. However, the criterion of the longest frustrated exchange bonds permits one to reduce significantly the range of the search for the state with the absolute minimum.
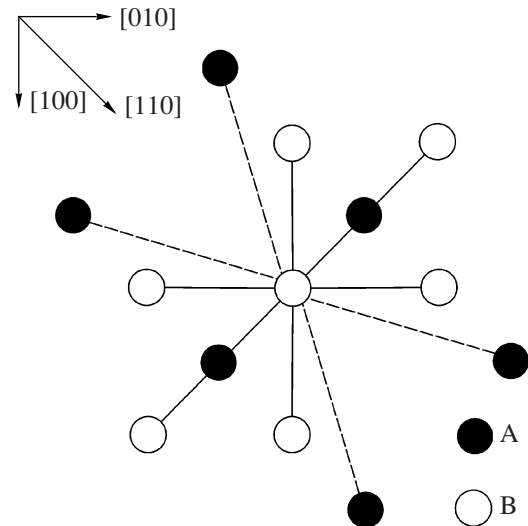
Fig. 8. Schematic drawing of the exchange bonds inside the antiferromagnetic subsystem (solid lines) and the intersubsystem bonds (dashed lines) in the structure of the normal cubic spinel.

ACKNOWLEDGMENTS

REFERENCES

1. Yu. A. Izyumov, *Neutron Diffraction in Long-Periodic Structures* (Énergoatomizdat, Moscow, 1987), pp. 27, 154 [in Russian].

2. H. Kawamura, J. Phys. Soc. Jpn. **54**, 3220 (1985); J. Phys. Soc. Jpn. **56**, 474 (1987).

3. V. P. Plakhty, J. Kulda, D. Visser, E. V. Moskvin, and J. Wosnitza, Phys. Rev. Lett. **85**, 3942 (2000).

4. T. Hikihara, M. Kaburagi, and H. Kawamura, Phys. Rev. B: Condens. Matter **63**, 174430 (2001).

5. T. A. Kaplan, Phys. Rev. **116**, 888 (1959); Phys. Rev. **119**, 1460 (1960).

6. D. H. Lyons and T. A. Kaplan, Phys. Rev. **120**, 1580 (1960).

7. T. A. Kaplan, K. Dwight, D. H. Lyons, and N. Menyuk, J. Appl. Phys. **32**, 13S (1961).

8. D. H. Lyons, T. A. Kaplan, K. Dwight, and N. Menyuk, Phys. Rev. **126**, 540 (1962).

9. N. Menyuk, K. Dwight, D. H. Lyons, and T. A. Kaplan, Phys. Rev. **127**, 1982 (1962).

10. S. Krupička, *Physik der Ferrite und der verwandten magnetischen Oxide* (Academia, Prague, 1973; Mir, Moscow, 1976), Vol. 1 [in German and in Russian].

11. S. M. Zhilyakov and E. P. Naĭden, *Magnetic Structure of Diamagnetically Diluted Cubic Ferrimagnets* (Tomsk University, Tomsk, Russia, 1990), p. 64 [in Russian].

12. R. Moessner and J. T. Chalker, Phys. Rev. Lett. **80**, 2929 (1998).

13. S.-H. Lee, C. Broholm, W. Ratcliff, G. Gasparovic, Q. Huang, T. H. Kim, and S.-W. Cheong, Nature (London) **418**, 856 (2002).

14. S. S. Sosin, L. A. Prozorova, and A. I. Smirnov, Usp. Fiz. Nauk **175** (1), 92 (2005) [Phys.—Usp. **48** (1), 83 (2005)].

15. N. P. Raju, M. Doim, M. J. Gingras, T. E. Mason, and J. E. Greedan, Phys. Rev. B: Condens. Matter **59**, 14489 (1999).

16. J. D. M. Champion, A. S. Wills, T. Fennell, S. T. Bramwell, J. S. Gardner, and M. A. Green, Phys. Rev. B: Condens. Matter **64**, 140407 (2001).

17. S. N. Martynov and A. D. Balaev, Pis'ma Zh. Éksp. Teor. Fiz. **85** (12), 785 (2007) [JETP Lett. **85** (12), 649 (2007)].

18. W. Zhang, W. M. Saslow, and M. Gabay, Phys. Rev. B: Condens. Matter **44**, 5129 (1991).

19. M. A. Popov, G. A. Petrakovskiĭ, and V. I. Zinenko, Fiz. Tverd. Tela (St. Petersburg) **46** (3), 478 (2004) [Phys. Solid State **46** (3), 491 (2004)].

20. I. E. Dzyaloshinskiĭ, Zh. Éksp. Teor. Fiz. **47**, 992 (1964) [Sov. Phys. JETP **20**, 665 (1964)].

21. T. Moriya, Phys. Rev. **120**, 91 (1960).

22. M. E. Zhitomirsky, Phys. Rev. B: Condens. Matter **52**, 353 (1996).

23. A. Pankrats, G. Petrakovskii, V. Tugarinov, K. Sablina, L. Bezmaternykh, R. Szymczak, M. Baran, B. Kundys, and A. Nabialek, J. Magn. Magn. Mater. **300**, e388 (2006).

24. M. E. Zhitomirsky, A. Honecker, and O. A. Petrenko, Phys. Rev. Lett. **85**, 3269 (2000).

25. A. P. Ramirez, B. S. Shastry, A. Hayashi, J. J. Krajewski, D. A. Huse, and R. J. Cava, Phys. Rev. Lett. **89**, 067202 (2002).

Translated by O. Borovik-Romanova